Toxoplasma gondii Co-opts the Unfolded Protein Response To Enhance Migration and Dissemination of Infected Host Cells

Leonardo Augusto,[a,b] Jennifer Martynowicz,[c] Parth H. Amin,[a] Nada S. Alakhras,[a] Mark H. Kaplan,[c] Ronald C. Wek,[a] William J. Sullivan, Jr.[b,c]

[a]Department of Biochemistry & Molecular Biology, Indiana University School of Medicine, Indianapolis, Indiana, USA
[b]Department of Pharmacology & Toxicology, Indiana University School of Medicine, Indianapolis, Indiana, USA
[c]Department of Microbiology & Immunology, Indiana University School of Medicine, Indianapolis, Indiana, USA

ABSTRACT *Toxoplasma gondii* is an intracellular parasite that reconfigures its host cell to promote pathogenesis. One consequence of *Toxoplasma* parasitism is increased migratory activity of host cells, which facilitates dissemination. Here, we show that *Toxoplasma* triggers the unfolded protein response (UPR) in host cells through calcium release from the endoplasmic reticulum (ER). We further identify a novel role for the host ER stress sensor protein IRE1 in *Toxoplasma* pathogenesis. Upon infection, *Toxoplasma* activates IRE1, engaging its noncanonical role in actin remodeling through the binding of filamin A. By inducing cytoskeletal remodeling via IRE1 oligomerization in host cells, *Toxoplasma* enhances host cell migration *in vitro* and dissemination of the parasite to host organs *in vivo*. Our study has identified novel mechanisms used by *Toxoplasma* to induce dissemination of infected cells, providing new insights into strategies for treatment of toxoplasmosis.

IMPORTANCE Cells that are infected with the parasite *Toxoplasma gondii* exhibit heightened migratory activity, which facilitates dissemination of the infection throughout the body. In this report, we identify a new mechanism used by *Toxoplasma* to hijack its host cell and increase its mobility. We further show that the ability of *Toxoplasma* to increase host cell migration involves not the enzymatic activity of IRE1 but rather IRE1 engagement with actin cytoskeletal remodeling. Depletion of IRE1 from infected host cells reduces their migration *in vitro* and significantly hinders dissemination of *Toxoplasma in vivo*. Our findings reveal a new mechanism underlying host-pathogen interactions, demonstrating how host cells are co-opted to spread a persistent infection around the body.

KEYWORDS *Toxoplasma*, parasites, UPR, IRE1, PERK, cell migration, filamin A, host-pathogen interactions, pathogenesis

*T*oxoplasma gondii is an obligate intracellular parasite capable of infecting any nucleated cell in warm-blooded vertebrates. Recent studies have revealed a striking degree of host cell remodeling taking place in *Toxoplasma*-infected cells that serves to facilitate pathogenesis and transmission. In addition to secreted parasite effectors that modulate host cell gene expression, *Toxoplasma* infection can alter immune responses and enable dissemination to other host tissues (1). Therein, *Toxoplasma* can differentiate from the replicative tachyzoites to the latent bradyzoite stage, enabling formation of tissue cysts that persist for the lifetime of the infected host (2).

Upon host cell invasion, *Toxoplasma* forms a parasitophorous vacuole (PV) that serves as a protective niche that can interface with the host cell cytoplasm to sequester nutrients (3). Curiously, *Toxoplasma* recruits the host endoplasmic reticulum (ER) to the PV via association between their respective membranes, although the reasons for this high-affinity interaction are not yet understood (4, 5).

The ER is sensitive to the perturbations in protein homeostasis through a stress-sensing pathway known as the unfolded protein response (UPR). Three ER transmembrane proteins, IRE1, ATF6, and PERK, operate as sensors that activate the UPR, leading to changes in gene expression that restore and expand the processing capacity of the organelle (6–8). IRE1 (ERN1) is a protein kinase and endoribonuclease that facilitates cytosolic splicing of *XBP1* (XBP1s) mRNA, thereby enhancing expression of the XBP1s isoform, which induces transcription of genes involved in ER-associated protein degradation (ERAD), lipid synthesis, and protein folding (7, 8). In response to ER stress, ATF6 transits from the ER to the Golgi apparatus, where it is cleaved, releasing an N-terminal cytosolic fragment (ATF6-N) that enters the nucleus and activates UPR target genes involved in protein folding and transport (6, 9). PERK (EIF2AK3) is the third UPR sensor, which phosphorylates the α subunit of eukaryotic initiation factor 2 (eIF2α) to direct translational and transcriptional modes of gene expression that regulate ER processing of proteins, metabolism, and the oxidation status of cells (6, 10). While the three ER stress sensory proteins function in parallel, there is cross-regulation that serves to coordinate the timing and magnitude of the UPR. For example, PERK was reported to induce expression of RPAP2, which serves to dephosphorylate and repress IRE1, thereby providing a means for the cell to abort failed ER stress adaptation and trigger apoptosis (11).

In addition to its role in the UPR, IRE1 was recently shown to modulate cytoskeletal remodeling and cell migration through direct interactions with the actin cross-linking factor filamin A (12). The role of IRE1 in cytoskeletal remodeling is enhanced by pharmacological induction of ER stress but occurs independently of IRE1 protein kinase and endoribonuclease activities (12); rather, IRE1 serves as a scaffolding protein for filamin A to orchestrate changes in cellular motility. This is noteworthy because *Toxoplasma* stimulates host cell migration, turning its host cell into a "Trojan horse" that can ferry parasites throughout the body (13). Given the recruitment of host ER to the PV, we postulated that migratory activities mediated by IRE1 function in parasite dissemination. In the present study, we uncovered a new mechanism by which *Toxoplasma* alters host ER homeostasis to produce hypermigratory activity in infected host cells. We show that during the course of *Toxoplasma* infection, the three UPR sensory proteins in the host cells are activated by a process involving calcium release from the ER, leading to IRE1 oligomerization, association with filamin A, and enhanced cell migration. Importantly, the IRE1-associated migration is a crucial determinant for successful dissemination of toxoplasmosis in a mouse model of infection.

RESULTS

Induction of the UPR in *Toxoplasma*-infected host cells. It is currently unclear why intracellular tachyzoites recruit host ER to the parasite PV. To address whether *Toxoplasma* perturbs host ER homeostasis, we infected mouse embryonic fibroblasts (MEFs) with RH strain parasites and measured three primary markers of the host UPR over a 36-h time course. Within 12 h of infection, *Toxoplasma* increased activation of PERK as measured by its self-phosphorylation (PERK-P), induced expression of ATF6 and formation of its cleavage product ATF6-N, and increased levels of the IRE1-derived spliced variant of XBP1 (XBP1s) (Fig. 1A). It is noteworthy that whereas expression of ATF6-N and XBP1s was transient, with increased amounts of the proteins appearing between 12 and 20 h postinfection (hpi), PERK-P increased throughout the 36 h of infection (Fig. 1A). These results indicate that *Toxoplasma* infection causes ER stress that activates each of the sensory proteins of the UPR, with some differences in the duration of their induction.

Activation of IRE1 involves oligomerization that can be visualized by a pattern of punctate spots by IFA (14–16). We expressed enhanced green fluorescent protein (EGFP)-tagged IRE1 in MEFs that had deletions of the endogenous *IRE1* gene by CRISPR/Cas9 genome editing (see Fig. S1A to C in the supplemental material); upon *Toxoplasma* infection, we observed formation of IRE1 foci, which is consistent with reported IRE1 activation by oligomerization (Fig. 1B) (15, 16). Furthermore, expres-
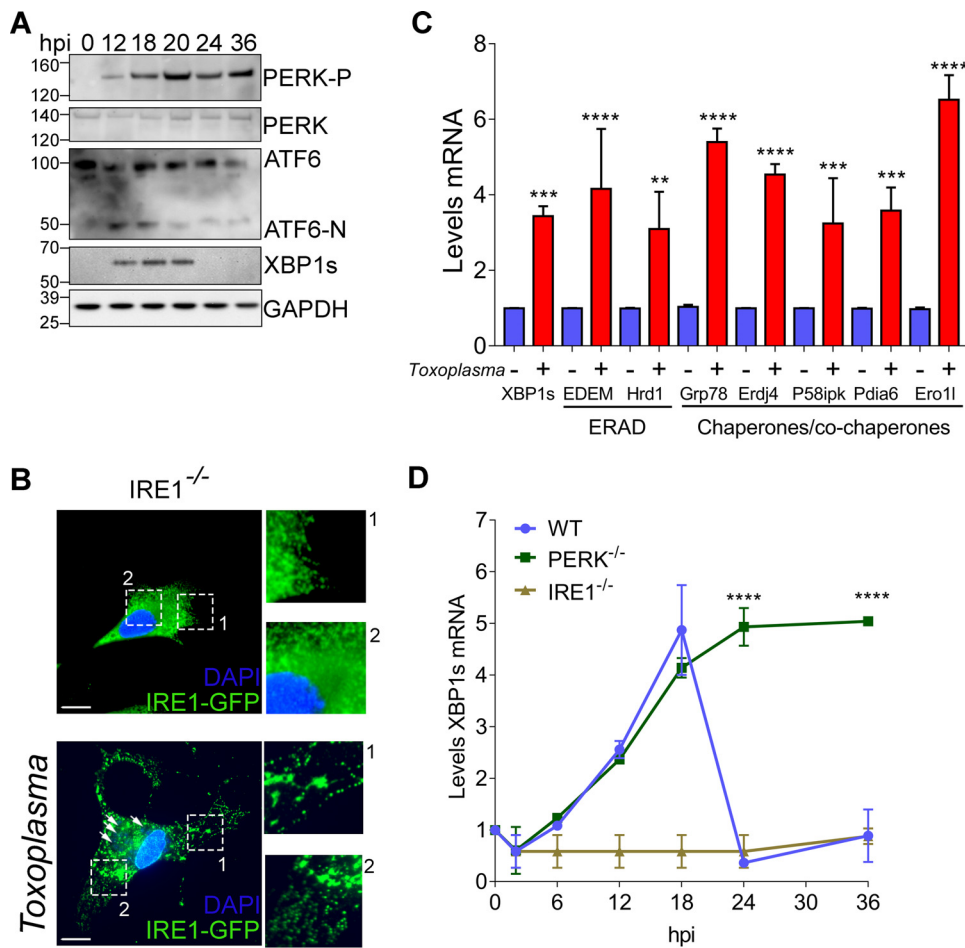
FIG 1 *Toxoplasma* infection triggers activation of the UPR in host cells. (A) At the indicated times following infection with *Toxoplasma*, cells were harvested and the levels of total PERK, PERK-P, full-length ATF6 and ATF6-N, XBP1s, and GAPDH were measured by immunoblot analyses. (B) *IRE1*$^{-/-}$ MEFs were transfected with a plasmid encoding EGFP-IRE1 (green), followed by infection with *Toxoplasma*. DAPI (blue) was used to visualize host cell and parasite nuclei. Two boxed areas (1 and 2) of each condition are amplified to highlight the IRE1 distribution. Bar = 5 μm. Arrows indicate *Toxoplasma* infection as based on DAPI staining. (C) MEFs were infected with *Toxoplasma* for 18 h, or were mock infected, and the mRNA levels of the indicated ERAD/chaperone genes were measured by RT-qPCR. Levels of mRNA were normalized to those for mock-infected cells, represented as a value of 1 ($\pm$SD; $n = 3$). **, $P < 0.005$; ***, $P < 0.001$; ****, $P < 0.0001$. (D) *XBP1s* mRNA levels were measured by RT-qPCR at the indicated times in WT, *PERK*$^{-/-}$, and *IRE1*$^{-/-}$ MEFs, as indicated. Levels of *XBP1s* mRNA were normalized to total *XBP1* mRNA in mock-infected cells (value of 1) at each time point ($\pm$SD; $n = 3$). ****, $P < 0.0001$.

sion of *XBP1s* mRNA, and its downstream target genes involved in ERAD and protein folding, was induced upon *Toxoplasma* infection of wild-type (WT) MEFs (Fig. 1C). These results indicate that IRE1 activation and signaling occur in response to *Toxoplasma* infection.

To further study the timing of UPR induction and potential cross-regulation between the UPR sensors in infected cells, we measured *XBP1s* mRNA levels by reverse transcription-quantitative PCR (RT-qPCR) in WT, *IRE1*$^{-/-}$, and *PERK*$^{-/-}$ MEFs. In WT cells, levels of *XBP1s* mRNA rose sharply until 18 hpi (Fig. 1D), consistent with the increase in XBP1s protein (Fig. 1A). As expected, *XBP1s* mRNA was not detected in infected *IRE1*$^{-/-}$ cells (Fig. 1D). In comparison, there was induced *XBP1s* mRNA that was sustained during 36 h of *Toxoplasma* infection in *PERK*$^{-/-}$ cells, indicating that without PERK, IRE1 continues to facilitate *XBP1s* expression (Fig. 1D). These results are consistent with the idea that PERK governs IRE1 activity, as previously reported (11), and suggest that in infected WT cells, PERK operates to attenuate the response of IRE1 after 18 hpi.
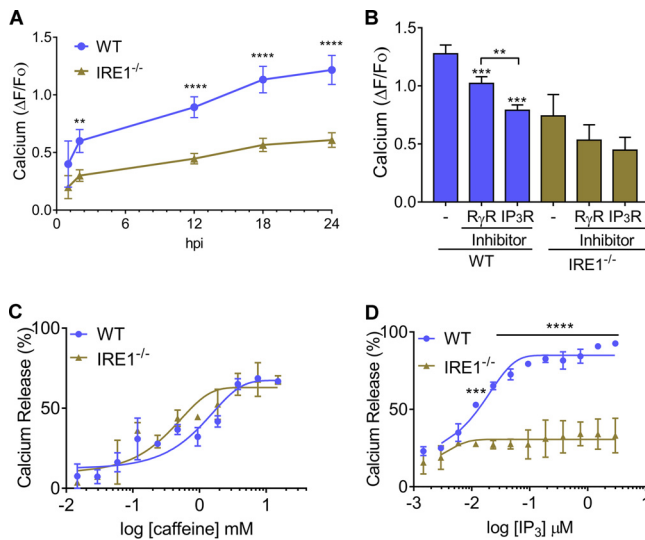
FIG 2 *Toxoplasma* infection induces calcium release. (A) At the indicated time, cytosolic calcium levels were measured in infected WT and *IRE1*$^{-/-}$ cells. Values of infected cells were normalized to those for mock-infected cells ($\pm$SD; $n = 3$). **, $P < 0.005$; ****, $P < 0.001$. (B) Infected WT and *IRE1*$^{-/-}$ cells were treated with RyR inhibitor (100 μM ryanodine) or IP$_3$R inhibitor (0.6 μM xestospongin C [XeC]) for 6 h, and the levels of cytosolic calcium were measured ($\pm$SD; $n = 3$). **, $P < 0.05$; ***, $P < 0.005$. Infected cells were incubated with Mag-Fluo-4, followed by plasma membrane permeabilization with saponin and incubation with ATP to maintain the calcium in the ER. To estimate RyR (C) and IP$_3$R (D) activities, WT and *IRE1*$^{-/-}$ cells infected with *Toxoplasma* for 18 h were treated with caffeine or IP$_3$ at the indicated concentrations; calcium release was represented as fluorescence using Mag-Fluo-4 as described previously (19). Values are percent calcium release; the respective start points were normalized to those for untreated WT and *IRE1*$^{-/-}$ cells, respectively ($\pm$SD; $n = 3$). **, $P < 0.05$; ****, $P < 0.001$.

IRE1 affects calcium release from ER in *Toxoplasma*-infected cells. Protein folding in the ER is highly sensitive to the concentration of calcium, which is released from the organelle by ryanodine receptors (RyR) and inositol 1,4,5-triphosphate (IP$_3$) receptors (IP$_3$R) (17). The ER is a major reservoir of calcium; disruptions of calcium homeostasis can lead to unfolded proteins and initiation of the UPR (17). To determine whether calcium content is altered in the host ER during *Toxoplasma* infection, we first measured cytosolic calcium in infected MEFs. Over an 18-h period, *Toxoplasma* infection induced a steady increase in host cell cytosolic calcium levels (Fig. 2A and Fig. S2A). Basal calcium levels in the cytosol of *IRE1*$^{-/-}$ cells were lower than in WT cells, as previously reported (18), with some increase upon parasite infection (Fig. 2A and Fig. S2A). To assess the mode of calcium release from the host ER during infection, we monitored calcium transport using fluorescent-4 acetoxymethyl ester (Fluo-4AM) in the presence of antagonists of RyR or IP$_3$R. The cytosolic calcium levels were lower in infected cells treated with either antagonist, with the most robust calcium reduction occurring with inhibition of IP$_3$R (Fig. 2B). We further addressed the contribution of RyR and IP$_3$R to calcium release by adding increasing doses of caffeine and IP$_3$, agonists of RyR and IP$_3$R activity (19), respectively, to WT and *IRE1*$^{-/-}$ cells infected with *Toxoplasma* for 18 h and incubated with Mag-Fluo-4. To compare calcium release between RyR and IP$_3$R in WT and *IRE1*$^{-/-}$ cells, the fluorescence values were represented as the percentage of calcium release and the respective start points were normalized to those for untreated WT and *IRE1*$^{-/-}$ cells, respectively. The RyR agonist enhanced calcium to similar levels in infected WT and *IRE1*$^{-/-}$ cells (Fig. 2C). In contrast, the agonist IP$_3$ induced appreciable calcium release only in infected WT cells (Fig. 2D), indicating a role for IRE1 in regulating IP$_3$R activity, as previously reported (18). Surprisingly, the percentage of calcium release was higher when IP$_3$R was stimulated than when RyR was stimulated, demonstrating that *Toxoplasma* infection differentially alters RyR and IP$_3$R activities. Collectively, these results suggest that *Toxoplasma* infection induces significant calcium release from the host ER by processes involving both IP$_3$R and RyR; this calcium release

is influenced by IRE1 and is a likely contributor to the activation of the host ER stress sensor proteins shown in Fig. 1A.

IRE1 activation induces cell migration in infected cells. *Toxoplasma* triggers rapid morphological changes in host cells, including disappearance of podosome structures and appearance of lamellipodia (20). IRE1 has recently been shown to have noncanonical functions in actin cytoskeletal remodeling by directly binding to filamin A (12). To address whether activation of IRE1 by *Toxoplasma* infection enhances host cell migration, we quantified the number of lamellipodia per infected cell normalized to the value for uninfected cells (Fig. 3A and Fig. S3A). At 18 hpi, *Toxoplasma* infection increased the number of lamellipodia in WT cells and these structures were significantly diminished in IRE1-deficient cells (Fig. 3A). There were greater numbers of lamellipodia in PERK-deficient cells or those treated with a PERK inhibitor, consistent with the idea that PERK is a negative regulator of IRE1 (Fig. 3A). Of interest, treatment with inhibitors of IRE1, namely, $4\mu8c$, which interferes with endoribonuclease activity, and KIRA6, which blocks IRE1 protein kinase activity, did not change the number of lamellipodia compared with that in infected cells treated with a vehicle (Fig. 3A). These results indicate that IRE1 can control migration of *Toxoplasma*-infected cells independently of its known enzymatic activities.

The functions of filamin A in cytoskeleton dynamics and cell migration are dependent on phosphorylation of serine 2152 (S2152) (21). We detected a sharp increase in filamin A phosphorylation in MEFs infected with *Toxoplasma* for 18 h, which was not observed in host cells lacking IRE1 (Fig. 3B). To address whether there is an association between IRE1 and filamin A, we expressed Myc-tagged filamin A (Myc-FLNA) in WT MEFs. Following 18 h of *Toxoplasma* infection, we then performed an immunoprecipitation (IP) of the tagged filamin A, followed by immunoblot measurements of associated IRE1. There was enhanced association of IRE1 with filamin A in cells infected with the parasite compared to those left uninfected (Fig. 3C).

Next, we measured changes in host cell transmigration upon parasite infection and determined that there was a 2-fold increase in migration of WT MEFs upon infection with *Toxoplasma* (Fig. 3D and Fig. S3B). Increased host cell migration was observed regardless of whether the cells were infected with type I RH or type II ME49 strain parasites (Fig. S3C). In contrast, parasite infection did not induce migration of cells lacking IRE1. Levels of migration in infected WT MEFs treated with one of the IRE1 enzymatic inhibitors, KIRA6 and $4\mu8c$, or an ATF6 inhibitor (Ceapin-A7) were not significantly changed compared to those in untreated infected MEFs, nor were they altered in cells lacking the downstream IRE1 target XBP1 (Fig. 3D and Fig. S3B). Notably, *Toxoplasma*-induced migration of PERK-deficient cells or WT cells treated with PERK inhibitor was increased >2.5-fold upon parasite infection compared to that in infected cells with functional PERK (Fig. 3D and Fig. S3B). These results suggest that IRE1 plays a critical role in inducing migration of *Toxoplasma*-infected cells and that this migration is independent of the protein kinase and endoribonuclease activities of IRE1 and its downstream target *XBP1*. Furthermore, PERK is suggested to dampen both IRE1 functions in *XBP1* mRNA splicing and cell migration, which are induced upon *Toxoplasma* infection.

ER stress induces cell migration by mechanisms involving IRE1 oligomerization. To better understand the mechanisms by which IRE1 enhances host cell migration in response to *Toxoplasma* infection, we rescued the $IRE1^{-/-}$ cells by expressing WT or defined mutant versions of IRE1 (Fig. 3E and Fig. S4A). Equal amounts of the IRE1 proteins were expressed as judged by immunoblot and immunofluorescence analyses (Fig. S4B and C). As expected, *ire1-wt* rescued the migration capacity of infected cells (Fig. 3E and Fig. S3D). Expression of IRE1 defective in kinase (*ire1-kD*) or endoribonuclease (*ire1-eD*) activities still rescued the migration phenotype, further supporting the idea that these activities are dispensable for induced cell migration in response to parasite infection (Fig. 3E). In contrast, cells expressing IRE1 with mutations in the oligomerization domain (*ire1-oD*) were deficient in *Toxoplasma*-induced migration
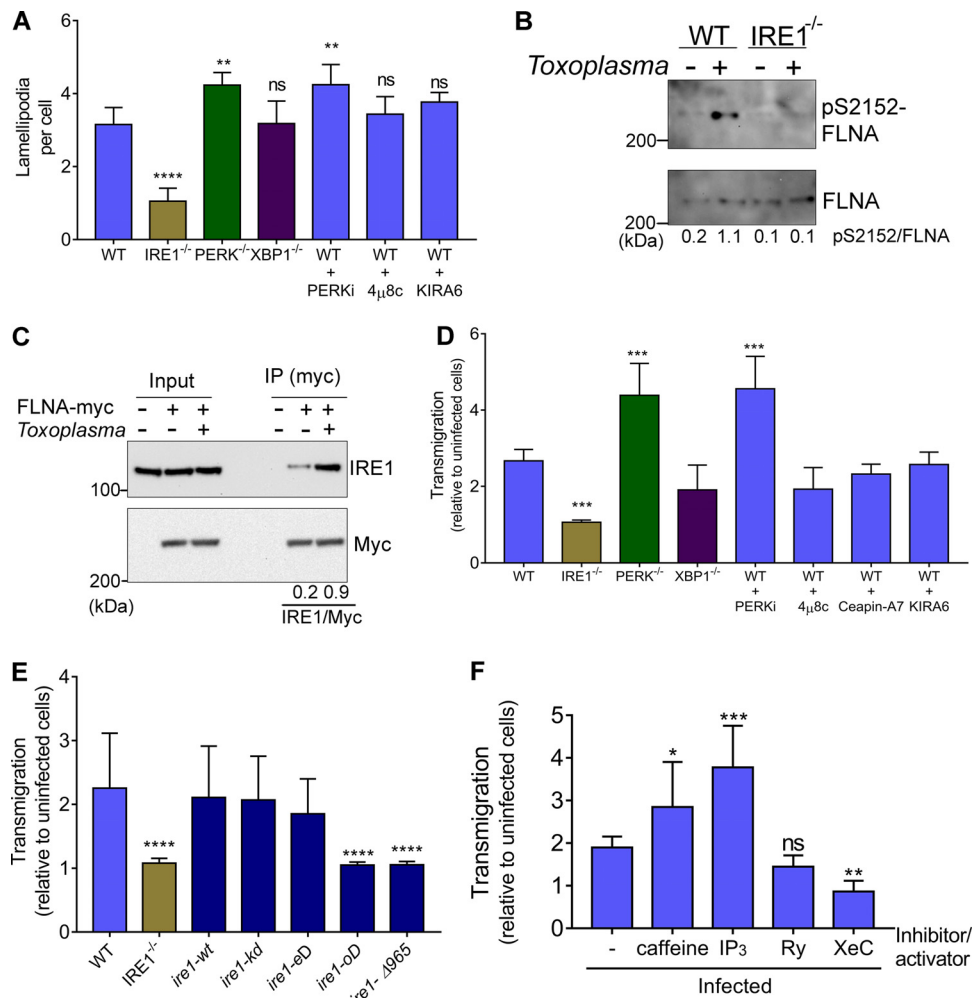
FIG 3 Activation of IRE1 enhances migration of cells infected with *Toxoplasma*. (A) The numbers of lamellipodia were determined in 50 randomly selected MEFs infected with *Toxoplasma* 18 hpi and normalized to uninfected cells. Also shown are infected WT cells treated with 1.2 μM PERKi (GSK2656157), 0. 4 μM 4μ8c, 250 nM KIRA6, or 0.2 μM ceapin-A7 for 18 h ($\pm$SD; $n = 5$). **, $P < 0.05$; ****, $P < 0.005$. ns, not significant. (B) WT and *IRE1*$^{-/-}$ cells were infected with *Toxoplasma* for 18 h, and then cells were harvested and the levels of filamin A phosphorylation (S2152) were measured by immunoblot analyses. (C) WT cells transiently expressing Myc-filamin A were infected with *Toxoplasma* for 18 h. IP of the tagged Filamin A was carried out using Myc magnetic beads. Bound proteins were separated by SDS-PAGE and the levels of Myc-filamin A and associated IRE1 were measured by immunoblotting and compared to those in uninfected cells. Densitometry of the IRE1 signal was divided by that of the Myc signal (IRE1/Myc). (D) WT or *IRE1*$^{-/-}$, *PERK*$^{-/-}$, and *XBP1*$^{-/-}$ cells were infected with *Toxoplasma* for 18 h. Alternatively, WT cells were infected with parasites and treated with the following inhibitors during migration per 18 h: 1.2 μM PERKi (GSK2656157), 0.2 μM Ceapin-A7, 250 nM KIRA6, or 0.4 μM 4μ8c. Infected and mock-infected cells were trypsinized and counted, and the same number of cells was used for the transmigration assay. Transmigration was determined by counting the number of infected normalized to noninfected cells that migrated through the membrane under each condition ($\pm$SD; $n = 3$). ***, $P < 0.0005$. (E) *IRE1*$^{-/-}$ cells were rescued with *ire1-wt* (wild type), *kD* (kinase domain dead; K599A), *eD* (endoribonuclease domain dead; P830L), *oD* (oligomerization domain dead; D123P), or $\Delta965$ (carboxy-terminally truncated $\Delta965$), and then a transmigration assay was carried out as described above ($\pm$SD; $n = 3$). ****, $P < 0.0001$. (F) Transmigration assay of infected WT MEFs was carried out in the presence of IP$_3$R and RyR inhibitors (0.6 μM XeC and 100 μM ryanodine [Ry]) or activators (100 μM IP$_3$ and 1 mM caffeine) ($\pm$SD; $n = 3$). *, $P < 0.1$; **, $P < 0.05$; ***, $P < 0.0005$.

(Fig. 3E). Furthermore, a truncated version of IRE1 (*ire1-Δ965*) lacking the proline-rich carboxy-terminal segment of IRE1 that binds filamin A (12) was also impaired in cell migration following infection (Fig. 3E). As anticipated, only *ire1-wt* and *ire1-Δ965* showed induction of spliced *XBP1* mRNA upon pharmacological induction of ER stress (Fig. S4D). These results suggest that *Toxoplasma* infection induces IRE1 oligomerization (see also Fig. 1B) and that the hypermigratory behavior of infected host cells is

reliant on both the oligomerization domain and the portion of IRE1 that interacts with filamin A.

Since we found that *Toxoplasma* induces calcium release from the host ER upon infection, we examined the importance of calcium release in host cell migration induced by *Toxoplasma*. We treated infected cells with RyR and IP_3R blockers or activators during the migration assay: ryanodine and xestospongin-C (XeC) were used to inhibit RyR and IP_3R, respectively; caffeine and IP_3 were used to activate RyR and IP_3R, respectively. When infected cells were treated with the RyR and IP_3R activators (releasing calcium from ER into the cytosol), the migration levels increased compared to those in cells not treated with these agents. In contrast, addition of the IP_3R inhibitor significantly decreased migration of the infected cells (Fig. 3F and Fig. S3E), consistent with IP_3R being the major calcium release receptor involved in triggering the host UPR following *Toxoplasma* infection (Fig. 2B). These results support the idea that calcium release from the host ER contributes to IRE1 activation and its subsequent role in augmenting migration in response to infection.

IRE1 controls host cell migration in infected immune cells *in vitro*. *Toxoplasma* makes use of immune cells as a "Trojan horse" to disseminate to distal organs and tissues throughout the body of the infected host (13). To address whether *Toxoplasma* targets IRE1 in immune cells to enhance their migration and facilitate dissemination, we infected bone marrow-derived dendritic cells (DCs) with *Toxoplasma*. Levels of *XBP1s* mRNA were sharply increased upon *Toxoplasma* infection in DCs (Fig. 4A), consistent with the idea that the parasite infection activated IRE1 in this cell type. Next, we used CRISPR/Cas9 and two distinct single guide RNAs (sgRNA1 and -2) to disrupt IRE1 in DCs (Fig. S5A). sgRNA1 and sgRNA2 decreased *IRE1* mRNA levels by 66% and 93%, respectively (Fig. 4B). Each gRNA also led to a corresponding reduction in IRE1 protein in DCs, with sgRNA2 leading to no detectable IRE1 (Fig. 4C). IRE1-depleted DCs [ire1 (−)] did not exhibit decreased viability compared to that of WT cells, nor did they show any difference in infectivity with *Toxoplasma* (Fig. 4D and Fig. S5B). However, loss of IRE1 in DCs significantly lowered the transmigratory capacity following infection with either type I or type II strains of *Toxoplasma* (Fig. 4E and Fig. S5C and D). To determine whether IP_3R plays a role in the migration of infected DCs, we carried out the migration assay in the presence of XeC. Inhibition of IP_3R resulted in a loss of host cell migration following 18 h of *Toxoplasma* infection (Fig. 4F and Fig. S5E), further supporting the importance of calcium homeostasis in the ER for migration of *Toxoplasma*-infected cells. To test whether IRE1 controls the migration of infected macrophages as well, we used CRISPR/Cas9 to deplete IRE1 in J774.1 macrophages (Fig. 4G and H). As observed for DCs, the loss of IRE1 significantly reduced the ability of infected macrophages to migrate (Fig. 4I and Fig. S5F).

IRE1 facilitates dissemination of *Toxoplasma in vivo*. To determine the importance of IRE1 in the migration of infected DCs *in vivo*, we inoculated C57BL/6 mice intraperitoneally (i.p.) with infected WT or infected ire1 (−) DCs and measured parasite burden in the spleen by PCR at various intervals over 3 days. Depletion of IRE1 in the DCs by CRISPR/Cas9 was confirmed by RT-qPCR and immunoblot analyses (Fig. 5A and B). Moreover, we ascertained that the depletion of IRE1 in DCs had no significant effect on parasite infectibility or replication rate (Fig. 5C and Fig. S5G). *Toxoplasma* was first detected in the spleens of mice 12 h following i.p. inoculation with infected WT DCs, increasing at each time point over the 3-day period (Fig. 5D). In striking contrast, appreciable levels of *Toxoplasma* dissemination of infected IRE1-depleted DCs to the spleen were not detected until 3 days following inoculation of the mice (Fig. 5D). Even at the 3-day point, the loss of IRE1 from DCs produced lowered levels of parasitemia in the spleen that were similar to those measured at 12 h for infected WT DCs. We also measured *Toxoplasma* dissemination to the brain at 3 days, finding 200-fold fewer parasites when infected IRE1-depleted DCs were inoculated into the mice (Fig. 5E). Mice inoculated with infected DCs lacking IRE1 survived significantly longer than mice receiving infected WT DCs (Fig. 5F). These results demonstrate a novel role for host IRE1
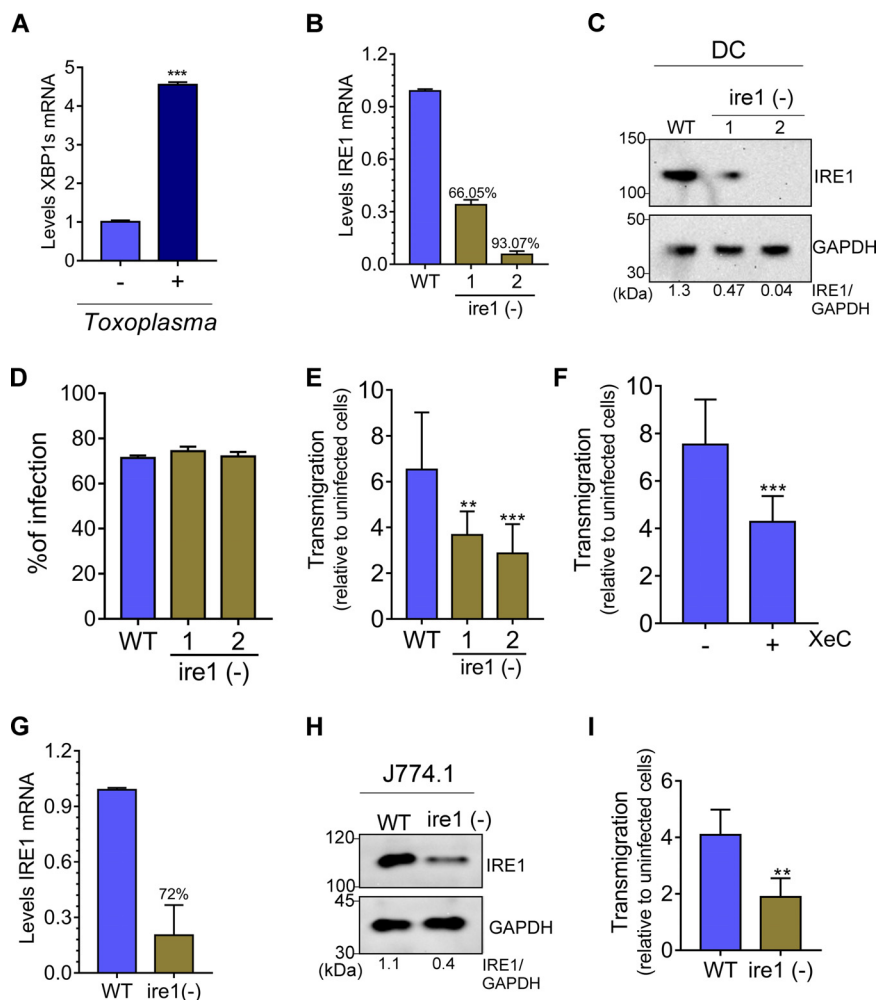
FIG 4 IRE1 is important for migration of infected DCs. (A) Bone marrow-derived DCs were infected with *Toxoplasma* for 18 h and *XBP1s* mRNA levels were measured by RT-qPCR. The values of *XBP1* transcripts were normalized to values of total XBP1 ($\pm$SD; $n = 3$). ***, $P < 0.0005$. (B and C) The CRISPR/Cas9-engineered depletion of IRE1 in DCs, designated ire1 ($-$), was assayed by RT-qPCR and immunoblotting using IRE1 antibody compared to WT cells (GAPDH was included as a loading control). (D) Percent infection was determined by counting the number of parasites inside 100 WT or ire1 ($-$) cells. (E) WT and ire1 ($-$) cells were infected for 18 h and the transmigration assay was carried out for 6 h. Transmigration was determined by counting the number of infected cells normalized to that of uninfected cells ($\pm$SD; $n = 3$). **, $P < 0.05$; ***, $P < 0.0005$. (F) WT DCs were infected for 18 h and the transmigration assay was carried out in the presence of 0.6 μM xestospongin C (XeC) for 6 h ($\pm$SD; $n = 3$). ***, $P < 0.001$. (G and H) J774.1 macrophages were transfected with sgRNA2 and the depletion of IRE1 was assayed by RT-qPCR and immunoblotting as described for panel C. (I) At 18 hpi, WT or ire1 ($-$) J774.1 macrophages were assayed for transmigration as described above ($\pm$SD; $n = 3$). **, $P < 0.05$.

in parasite pathogenesis, as IRE1 is crucial for the migration of immune cells being co-opted as Trojan horses for parasite dissemination.

DISCUSSION

Obligate intracellular pathogens create a niche inside their host cell that allows for parasite protection, nutrient acquisition, and the controlled release of pathogen effectors that promote infection and dissemination. *Toxoplasma* tachyzoites reside inside a nonfusogenic parasitophorous vacuole (PV) that forms intimate contacts with host organelles and vesicles, including the ER and mitochondria (4, 5). It is suggested that the recruitment of host organelles to the PV allows *Toxoplasma* to control critical host cell operations, including antigen presentation, nutrient production, and suppression of apoptosis (5). In this study, we addressed the consequences of the *Toxoplasma*-ER engagement on parasite infection and dissemination in the host. As illustrated in a
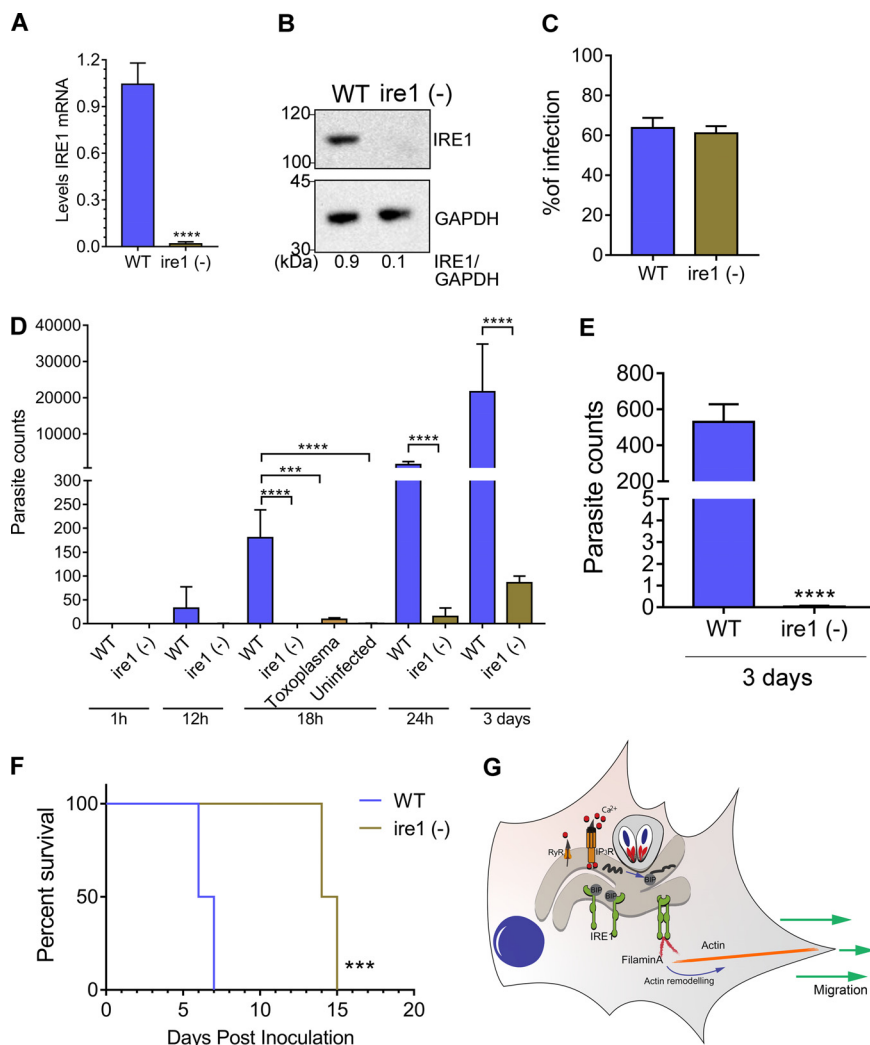
FIG 5 IRE1 facilitates migration of infected DCs *in vivo*. (A and B) IRE1 was depleted in bone marrow-derived DCs by CRISPR/Cas9, and loss of *IRE1* expression was assayed by RT-qPCR and immunoblot analyses. (C) WT or ire1 (−) DCs were infected for 18 h, and the percent infection was determined by counting the number of parasites in 100 cells. (D) Infected WT and ire1 (−) cells were inoculated into mice by intraperitoneal (i.p.) injection (10⁶ infected cells); mice infected i.p. with free tachyzoites in sterile PBS (RH strain) are designated "*Toxoplasma*." At the indicated hpi, the spleen of each mouse was harvested, and the number of parasites was determined by PCR. ***, $P < 0.005$; ****, $P < 0.0001$. (E) At 3 days postinoculation, the number of parasites in the brain was determined using PCR. ****, $P < 0.0001$. (F) Survival of C57BL/6 mice challenged with 10⁶ infected WT or ire 1 (−) DCs. ***, $P < 0.0005$. Statistical analyses were done by Gehan-Breslow-Wilcoxon test. (G) Model for IRE1 direct hypermigration of host cells infected by *Toxoplasma*. During infection, *Toxoplasma* triggers calcium release from the host ER, which creates ER stress and induction of the UPR, which results in enhanced IRE1 association with filamin A. Consequently, the IRE1-filamin A interaction promotes actin remodeling and host cell migration.

model presented in Fig. 5G, we showed that *Toxoplasma* infection activates each of the UPR sensor proteins, including IRE1, via ER stress that results at least in part from release of calcium from the organelle, primarily through IP$_3$R. In addition to its role in the UPR, IRE1 has recently been shown to have noncanonical functions associated with the remodeling of the cytoskeleton through direct interactions with the actin cross-linking factor filamin A (12). We showed that *Toxoplasma* alters the morphology of its host cells through IRE1-filamin A interactions, which directs cytoskeletal remodeling that contributes to a hypermigratory phenotype that facilitated dissemination of the parasite into multiple organs of the infection host. The role of IRE1 in *Toxoplasma*-induced hypermigration is not reliant on its protein kinase or endoribonuclease activities that are central for classical UPR signaling; rather, it is IRE1 oligomerization and the carboxy-

terminal residues required for filamin A association that prove to be important. Further mechanistic details into how ER recruitment to the PV elicits host UPR remain to be resolved.

After oral infection, *Toxoplasma* rapidly spreads from the lamina propria to distal organs using host immune cells as a vehicle for dissemination (22). Given our discovery that IRE1 is mobilized by *Toxoplasma* to enhance hypermigratory behavior in host cells, we tested whether IRE1 is crucial to *in vivo* dissemination in a mouse model of infection. We found that depletion of IRE1 in immune cells sharply decreases the number of parasites in the spleens or brains of infected mice (Fig. 5E). These results reveal a number of potential new targets for drug development aimed at thwarted spread of infection in the body.

It is noteworthy that other mechanisms have been suggested to contribute to the cell hypermotility upon *Toxoplasma* infection. For example, parasite effector protein TgWIP, TIMP-1, and GABAergic signaling was reported to signal hypermigration of certain infected host cells (23–26). A key question for future studies is how these different mechanisms are coordinated to induce hypermigratory activity in *Toxoplasma*-infected host cells.

MATERIALS AND METHODS

Host cell and parasite culture. Mouse embryonic fibroblasts (MEFs) were cultured in Dulbecco's modification of Eagle's medium (DMEM) supplemented with 10% heat-inactivated fetal bovine serum (FBS) (Gibco/Invitrogen) and penicillin-streptomycin at 37°C with 5% CO_2. $PERK^{-/-}$ cells were previously reported (27), and IRE1-deficient MEFs were engineered by CRISPR as described below. Host cells were seeded at a density of 2×10^5/well in a 6-well plate and cultured for 18 h. Infection was performed using a multiplicity of infection (MOI) of 3 with type I or II (RH or ME49) strain *Toxoplasma* parasites for 18 h. The infected cells were cultured in DMEM supplemented with 10% heat-inactivated FBS (Gibco/Invitrogen) and penicillin-streptomycin at 37°C with 5% CO_2. Cultures of DCs and J774.1 macrophages were cultivated in RPMI medium supplemented with 10% heat-inactivated FBS (Gibco/Invitrogen) and penicillin-streptomycin at 37°C with 5% CO_2 and infected as described above.

Generation of *IRE1* knockout cells. Disruption of the *IRE1* gene in MEFs was carried out using the CRISPR/Cas9 method (28). Two distinct sgRNAs designed using DESKGEN toll (g1-TGGACACGGAGCT GACT and g2-ACACGGAGCTGACTGGG) were examined individually. The sgRNAs were prepared using the EnGen sgRNA synthesis kit (New England BioLabs), along with an sg control (g-control-CATCCTCGGCA CCGTCACCC). The sgRNAs were then associated with EnGen Spy Cas9 NLS protein (New England BioLabs) at room temperature for 20 min. MEFs were then transfected with the bound sgRNA/Cas9 protein using the Lipofectamine CRISPRMAX Cas9 transfection reagent (Thermo Fisher Scientific). After culturing the transfected cells for 48 h, 100 cells were plated in 10-mm tissue-culture dishes for cloning. Cloned $IRE1^{-/-}$ MEFs were validated by RT-qPCR using specific primers and by immunoblotting using IRE1-specific antibody (Abcam; ab37073). $IRE1^{-/-}$ cells were complemented with pcDNA3-derived vectors containing WT or mutant versions of *IRE1*. Briefly, the mouse cDNA sequence of *IRE1* from MEFs was inserted into pcDNA3-EGFP plasmid (Addgene; number 13031), resulting in fusion proteins with EGFP fused to the carboxy terminus of IRE1. Mutations in *IRE1* include changes inactivating the critical functions, including kD (kinase domain; K599A), eD (endoribonuclease domain; P830L), oD (oligomerization domain; D123P), and c-terminal (carboxy-terminally truncated Δ965), were carried out using specific primers (Table S1) and the Q5 site-directed mutagenesis kit (New England BioLabs). After sequence verification, the plasmids were transfected into $IRE1^{-/-}$ cells using FuGENE 6 transfection reagent. Rescued WT and mutant IRE1 protein expression were confirmed by immunoblotting and immunofluorescence microscopy (Fig. S4A to C).

To generate bone marrow-derived dendritic cells (DCs), 10×10^6 bone marrow cells were isolated and cultured in a 6-well plate in 3 ml of complete medium (RPMI 1640 medium supplemented with 10% fetal bovine serum, penicillin, streptomycin, glutamine, 2-mercaptoethanol, 20 ng/ml of granulocyte-macrophage colony-stimulating factor [GM-CSF], and 5 ng/ml of interleukin 4 [IL-4] [both from Pepro-tech]) for 7 days. Half of the medium was replaced every 2 days with medium supplemented with GM-CSF and IL-4, as previously described (29). DCs or J774.1 macrophages were transfected with IRE1-sgRNA1 or -2, associated with EnGen Spy Cas9 NLS protein (New England BioLabs), using the 4D-Nucleofector system (Lonza) in combination with the P3 Primary Cell 4D-Nucleofector X kit. After 48 h, the *IRE1* mRNA and protein levels were measured by RT-qPCR and immunoblotting, respectively. Viability of DCs was examined by trypan blue staining.

Measurement of mRNA levels. Cells were first infected with *Toxoplasma* for 2 h, washed with phosphate-buffered saline (PBS), and then cultured in DMEM at the desired time points. RNA was isolated from cells using TRIzol LS reagent (Invitrogen), the cDNA was then generated using Omniscript (Qiagen), and RT-qPCR was performed using SYBR green real-time PCR master mixes (Invitrogen) and the StepOnePlus real-time system (Applied Biosystems). Oligonucleotide primers used to measure each target mRNA are listed in Table S1. Relative levels of transcripts were calculated with the threshold cycle ($\Delta\Delta C_T$) method using genes encoding glyceraldehyde-3-phosphate dehydrogenase (GAPDH) and β-actin as internal controls, and then the relative levels of target mRNAs from the mock-infected samples were

adjusted to 1 and served as the basal control value. Values of each time point were normalized to mock infection. Each experiment was performed three times, each with three technical replicates.

Immunoblot analyses. Cells were infected with *Toxoplasma* for 2 h, washed with PBS, and then cultured in DMEM for the desired times. The infected cells were harvested in radioimmunoprecipitation assay (RIPA) buffer solution supplemented with cOmplete, EDTA-free protease inhibitor cocktail (Roche). Protein quantification was performed using Bradford reagent (Sigma-Aldrich). Equal amounts of protein lysates were separated by SDS-PAGE, and proteins were transferred to nitrocellulose filters. Immunoblot analyses were done using primary antibodies against IRE1 (Abcam; ab37073), XBP1s (Cell Signaling; number D2C1F), ATF6 (30), GAPDH (Abcam; ab9485), and PERK (Cell Signaling; number 3192), followed by Amersham ECL horseradish peroxidase (HRP)-conjugated secondary antibody. These antibodies and additional reagents used in the study are listed in Table S2. Proteins in the immunoblots were visualized using FluorChem M (multiplex fluorescence; Protein Simple). Immunoblot analyses were carried out for three independent experiments.

Calcium measurement assay. *Toxoplasma*-infected MEFs were washed twice with buffer A solution supplemented with glucose (120 mM NaCl, 20 mM HEPES [pH 7.4], 4.7 mM KCl, 1.2 mM NaH$_2$PO$_4$, 1.2 mM MgSO$_4$, 1.2 mM CaCl$_2$, and 10 mM glucose) (31), and then a final concentration of 5 μM Fluo-4AM (Thermo Fisher Scientific; F14201) was added for 15 min at 37°C. Prior to the calcium measurements, cells were washed once with buffer A solution supplemented with glucose. A Synergy (BioTek) plate reader was used to monitor the Fluo-4AM fluorescence at 488-nm excitation and 524-nm emission wavelengths. Values derived from infected cells (ΔF) were divided by the resting intracellular calcium (Fo), ΔF/Fo, and the values of each time point were normalized to the value for mock-infected cells. In parallel, live infected cells were imaged by microscopy at the same exposure and a heat map was generated using ImageJ software. To determine the activity of RyR and IP$_3$R, infected cells were incubated with 5 μM Mag-Fluo-4, a low-affinity Ca^{2+} indicator, and then permeabilized with 10 μg/ml of saponin followed by incubation with 1.5 mM ATP to maintain Mag-Fluo-4 in the ER (19) (Fig. S2B). Infected cells were treated with the desired concentrations of caffeine (RyR, 0 to 200 mM) or IP$_3$ (IP$_3$R, 0 to 3 μM) (Sigma-Aldrich). A Synergy (BioTek) plate reader was used to monitor the Mag-Fluo-4 fluorescence at 490-nm excitation and 525-nm emission wavelengths (19). Values were normalized to those of mock-infected cells.

Immunofluorescence assay. Cultured cells were infected with *Toxoplasma* for 18 h, then fixed with 2.5% paraformaldehyde for 20 min, and blocked with PBS supplemented with 2% bovine serum albumin (BSA). Cells were permeabilized in blocking solution containing 0.01% Triton X-100 for 30 min and incubated with primary antibody (SAG1-p30; Invitrogen) for 1 h. Secondary goat anti-rabbit Alexa Fluor 488 (Invitrogen) was applied for 1 h in the presence of rhodamine phalloidin (Thermo Fisher Scientific) followed by Prolong gold antifade reagent (Invitrogen). 4′,6-Diamidino-2-phenylindole (DAPI) was used to visualize host cells and parasite nuclei (Vector Labs). Images were acquired with a Leica inverted DMI6000B microscope with a 63× oil immersion objective and analyzed in ImageJ. Alternatively, *IRE1*$^{-/-}$ cells were transfected with pcDNA3 encoding IRE1 fused with EGFP at the carboxy terminus and infected with *Toxoplasma* for 18 h (MOI, 3); the cells were then fixed and imaged as described above.

Immunoprecipitation assay. The mouse cDNA sequence of filamin A from MEFs was amplified and cloned into pcDNA3-myc plasmid (Addgene). The resulting plasmid, pcDNA3-myc-FLNA, was transiently transfected in MEFs, and then the transfected cells were infected with *Toxoplasma* for 18 h (MOI, 3). Cell lysates were prepared using IP-lysis solution (0.5% NP-40, 250 mM NaCl, 30 mM Tris, 0.5% glycerol [pH 7.4], 250 mM phenylmethylsulfonyl fluoride [PMSF] supplemented with cOmplete, EDTA-free protease inhibitor cocktail [Roche]). To immunoprecipitate Myc-tagged filamin A (Myc-filamin A), equal amounts of protein lysates were incubated with IgG magnetic beads (Pierce) for 2 h and then mixed with anti-Myc magnetic beads (Pierce) overnight at 4°C with rotation. Proteins bound to the beads were subsequently washed four times with IP-lysis solution at 4°C and then once with IP-lysis solution supplemented with 500 mM NaCl. Protein complexes were eluted at 95°C for 5 min in loading buffer solution and then separated by SDS-PAGE, followed by immunoblot analyses using specific antibodies to IRE1 (Abcam; ab37073) or Myc (Cell Signaling; no. 2276).

Cell migration assay. Cells were infected with *Toxoplasma* at an MOI of 3 for 18 h and then trypsinized and counted using a hemocytometer; 2 × 10⁴ cells were resuspended in serum-free medium and applied to the top of a membrane coated with collagen I (rat tail) (Gibco; A1048301). Transmigration assays were carried out using a Corning Transwell Costar apparatus (6.5-mm diameter and 8-μm pore size) as described previously (32). After 18 h for MEFs and 6 h for DCs and macrophages, the medium was removed, and the cells were fixed with 2.5% paraformaldehyde for 20 min. To facilitate counting of migrated cells, cells that did not migrate and remained on the upper side of membrane (unmigrated cells) were removed with a swab. The membrane was incubated with Prolong gold antifade reagent with DAPI. Cells were counted using a Leica inverted DMI6000B microscope with a 63× oil immersion objective. The transmigration was determined by numbers of migrated infected cells in 5 fields normalized to number of uninfected cells in each cell type and treatment. Each transmigration assay was carried out in technical triplicate ($n = 3$).

***In vivo* migration assay.** DCs were plated in 6-well plates (1 × 10⁶ cells/well) and allowed to adhere overnight. DCs were infected with *Toxoplasma* for 1 h (MOI, 3) and then washed with RPMI medium to remove extracellular parasites. After 18 h, infected DCs were incubated with CellTracker Orange CMTMR (Thermo Fisher) as described previously (33). Infected DCs were intraperitoneally inoculated into 6-week-old female C57BL/6J mice whose spleens and brains were subsequently harvested at the indicated time points. DC migration to the spleen was measured by fluorescence intensity using a Synergy (BioTek) plate reader at excitation and emission wavelengths of 541 and 565 nm (Fig. S5H). Also, DNA was isolated from the spleen and brain using TRIzol (Thermo Fisher), and the number of parasites was determined by using

a PCR-based method measuring levels of the parasite-specific gene region B1 as previously described (34). After 3 days, the mice were observed twice a day and percent survival was recorded at each time point. The mouse experiments, including parasite measurement by B1, were performed blinded. The mice used in this study were housed in American Association for Accreditation of Laboratory Animal Care (AAALAC)-approved facilities at the Indiana University School of Medicine Laboratory Animal Research Center (LARC). The Institutional Animal Care and Use Committee (IACUC) at Indiana University School of Medicine approved the use of all animals and procedures (IACUC protocol number 11376).

Quantification and statistical analysis. Quantitative data are presented as means and standard deviations and were derived from three biological replicates. Statistical significance was determined using one-way analysis of variance (ANOVA) with Tukey's *post hoc* test and multiple two-tailed *t* test using Graph Prism software. The number of biological replicates and *P* values are indicated in figure legends. For immunoblot analyses, the reported images are representative of at least three independent experiments. The mouse survival curve was analyzed by Gehan-Breslow-Wilcoxon test for *in vivo* analysis.

SUPPLEMENTAL MATERIAL

Supplemental material is available online only.

FIG S1, TIF file, 0.5 MB.
FIG S2, TIF file, 2.3 MB.
FIG S3, TIF file, 2 MB.
FIG S4, TIF file, 2.7 MB.
FIG S5, TIF file, 1.5 MB.
TABLE S1, DOCX file, 0.02 MB.
TABLE S2, DOCX file, 0.02 MB.

ACKNOWLEDGMENTS

REFERENCES

1. Hakimi M-A, Olias P, Sibley LD. 2017. *Toxoplasma* effectors targeting host signaling and transcription. Clin Microbiol Rev 30:615–645. https://doi.org/10.1128/CMR.00005-17.

2. Jeffers V, Tampaki Z, Kim K, Sullivan WJ. 2018. A latent ability to persist: differentiation in *Toxoplasma gondii*. Cell Mol Life Sci 75:2355–2373. https://doi.org/10.1007/s00018-018-2808-x.

3. Blader IJ, Koshy AA. 2014. *Toxoplasma gondii* development of its replicative niche: in its host cell and beyond. Eukaryot Cell 13:965–976. https://doi.org/10.1128/EC.00081-14.

4. Sinai AP, Webster P, Joiner KA. 1997. Association of host cell endoplasmic reticulum and mitochondria with the *Toxoplasma gondii* parasitophorous vacuole membrane: a high affinity interaction. J Cell Sci 110:2117–2128.

5. Coppens I, Romano JD. 2018. Hostile intruder: *Toxoplasma* holds host organelles captive. PLoS Pathog 14:e1006893. https://doi.org/10.1371/journal.ppat.1006893.

6. Walter P, Ron D. 2011. The unfolded protein response: from stress pathway to homeostatic regulation. Science 334:1081–1086. https://doi.org/10.1126/science.1209038.

7. Karagoz GE, Acosta-Alvear D, Walter P. 2019. The unfolded protein response: detecting and responding to fluctuations in the protein-folding capacity of the endoplasmic reticulum. Cold Spring Harb Perspect Biol 11:a033886. https://doi.org/10.1101/cshperspect.a033886.

8. Hetz C, Papa FR. 2018. The unfolded protein response and cell fate control. Mol Cell 69:169–181. https://doi.org/10.1016/j.molcel.2017.06.017.

9. Mori K. 2010. Divest yourself of a preconceived idea: transcription factor ATF6 is not a soluble protein! Mol Biol Cell 21:1435–1438. https://doi.org/10.1091/mbc.e09-07-0600.

10. Wek RC. 2018. Role of eif2alpha kinases in translational control and adaptation to cellular stress. Cold Spring Harb Perspect Biol 10:a032870. https://doi.org/10.1101/cshperspect.a032870.

11. Chang T-K, Lawrence DA, Lu M, Tan J, Harnoss JM, Marsters SA, Liu P, Sandoval W, Martin SE, Ashkenazi A. 2018. Coordination between two branches of the unfolded protein response determines apoptotic cell fate. Mol Cell 71:629–636.e5. https://doi.org/10.1016/j.molcel.2018.06.038.

12. Urra H, Henriquez DR, Cánovas J, Villarroel-Campos D, Carreras-Sureda A, Pulgar E, Molina E, Hazari YM, Limia CM, Alvarez-Rojas S, Figueroa R, Vidal RL, Rodriguez DA, Rivera CA, Court FA, Couve A, Qi L, Chevet E, Akai R, Iwawaki T, Concha ML, Glavic Á, Gonzalez-Billault C, Hetz C. 2018. IRE1alpha governs cytoskeleton remodelling and cell migration through a direct interaction with filamin A. Nat Cell Biol 20:942–953. https://doi.org/10.1038/s41556-018-0141-0.

13. Bierly AL, Shufesky WJ, Sukhumavasi W, Morelli AE, Denkers EY. 2008. Dendritic cells expressing plasmacytoid marker PDCA-1 are Trojan horses during *Toxoplasma gondii* infection. J Immunol 181:8485–8491. https://doi.org/10.4049/jimmunol.181.12.8485.

14. Korennykh AV, Egea PF, Korostelev AA, Finer-Moore J, Zhang C, Shokat

KM, Stroud RM, Walter P. 2009. The unfolded protein response signals through high-order assembly of Ire1. Nature 457:687–693. https://doi.org/10.1038/nature07661.

15. Aragon T, van Anken E, Pincus D, Serafimova IM, Korennykh AV, Rubio CA, Walter P. 2009. Messenger RNA targeting to endoplasmic reticulum stress signalling sites. Nature 457:736–740. https://doi.org/10.1038/nature07641.

16. Li H, Korennykh AV, Behrman SL, Walter P. 2010. Mammalian endoplasmic reticulum stress sensor IRE1 signals by dynamic clustering. Proc Natl Acad Sci U S A 107:16113–16118. https://doi.org/10.1073/pnas.1010580107.

17. Carreras-Sureda A, Pihán P, Hetz C. 2018. Calcium signaling at the endoplasmic reticulum: fine-tuning stress responses. Cell Calcium 70:24–31. https://doi.org/10.1016/j.ceca.2017.08.004.

18. Carreras-Sureda A, Jaña F, Urra H, Durand S, Mortenson DE, Sagredo A, Bustos G, Hazari Y, Ramos-Fernández E, Sassano ML, Pihán P, van Vliet AR, González-Quiroz M, Torres AK, Tapia-Rojas C, Kerkhofs M, Vicente R, Kaufman RJ, Inestrosa NC, Gonzalez-Billault C, Wiseman RL, Agostinis P, Bultynck G, Court FA, Kroemer G, Cárdenas JC, Hetz C. 2019. Noncanonical function of IRE1alpha determines mitochondria-associated endoplasmic reticulum composition to control calcium transfer and bioenergetics. Nat Cell Biol 21:755–767. https://doi.org/10.1038/s41556-019-0329-y.

19. Yamamoto WR, Bone RN, Sohn P, Syed F, Reissaus CA, Mosley AL, Wijeratne AB, True JD, Tong X, Kono T, Evans-Molina C. 2019. Endoplasmic reticulum stress alters ryanodine receptor function in the murine pancreatic beta cell. J Biol Chem 294:168–181. https://doi.org/10.1074/jbc.RA118.005683.

20. Weidner JM, Kanatani S, Hernández-Castañeda MA, Fuks JM, Rethi B, Wallin RPA, Barragan A. 2013. Rapid cytoskeleton remodelling in dendritic cells following invasion by *Toxoplasma gondii* coincides with the onset of a hypermigratory phenotype. Cell Microbiol 15:1735–1752. https://doi.org/10.1111/cmi.12145.

21. Zhou A-X, Hartwig JH, Akyürek LM. 2010. Filamins in cell signaling, transcription and organ development. Trends Cell Biol 20:113–123. https://doi.org/10.1016/j.tcb.2009.12.001.

22. Drewry LL, Sibley LD. 2019. The hitchhiker's guide to parasite dissemination. Cell Microbiol 21:e13070. https://doi.org/10.1111/cmi.13070.

23. Olafsson EB, Ross EC, Varas-Godoy M, Barragan A. 2019. TIMP-1 promotes hypermigration of *Toxoplasma*-infected primary dendritic cells via CD63-ITGB1-FAK signaling. J Cell Sci 132:jcs225193. https://doi.org/10.1242/jcs.225193.

24. Bhandage AK, Kanatani S, Barragan A. 2019. *Toxoplasma*-induced hypermigration of primary cortical microglia implicates GABAergic signaling. Front Cell Infect Microbiol 9:73. https://doi.org/10.3389/fcimb.2019.00073.

25. Bhandage AK, Barragan A. 2019. Calling in the CaValry—*Toxoplasma gondii* hijacks GABAergic signaling and voltage-dependent calcium channel signaling for Trojan horse-mediated dissemination. Front Cell Infect Microbiol 9:61. https://doi.org/10.3389/fcimb.2019.00061.

26. Sangare LO, Ólafsson EB, Wang Y, Yang N, Julien L, Camejo A, Pesavento P, Sidik SM, Lourido S, Barragan A, Saeij JPJ. 2019. In vivo CRISPR screen identifies TgWIP as a *Toxoplasma* modulator of dendritic cell migration. Cell Host Microbe 26:478–492.e8. https://doi.org/10.1016/j.chom.2019.09.008.

27. Jiang H-Y, Wek SA, McGrath BC, Lu D, Hai T, Harding HP, Wang X, Ron D, Cavener DR, Wek RC. 2004. Activating transcription factor 3 is integral to the eukaryotic initiation factor 2 kinase stress response. Mol Cell Biol 24:1365–1377. https://doi.org/10.1128/mcb.24.3.1365-1377.2004.

28. Cong L, Ran FA, Cox D, Lin S, Barretto R, Habib N, Hsu PD, Wu X, Jiang W, Marraffini LA, Zhang F. 2013. Multiplex genome engineering using CRISPR/Cas systems. Science 339:819–823. https://doi.org/10.1126/science.1231143.

29. Inaba K, Swiggard WJ, Steinman RM, Romani N, Schuler G. 2001. Isolation of dendritic cells. Curr Protoc Immunol Chapter 3:Unit 3.7.

30. Teske BF, Wek SA, Bunpo P, Cundiff JK, McClintick JN, Anthony TG, Wek RC. 2011. The eIF2 kinase PERK and the integrated stress response facilitate activation of ATF6 during endoplasmic reticulum stress. Mol Biol Cell 22:4390–4405. https://doi.org/10.1091/mbc.E11-06-0510.

31. Borges-Pereira L, Budu A, McKnight CA, Moore CA, Vella SA, Hortua Triana MA, Liu J, Garcia CRS, Pace DA, Moreno SNJ. 2015. Calcium signaling throughout the *Toxoplasma gondii* lytic cycle: a study using genetically encoded calcium indicators. J Biol Chem 290:26914–26926. https://doi.org/10.1074/jbc.M115.652511.

32. Lechuga S, Amin PH, Wolen AR, Ivanov AI. 2019. Adducins inhibit lung cancer cell migration through mechanisms involving regulation of cell-matrix adhesion and cadherin-11 expression. Biochim Biophys Acta Mol Cell Res 1866:395–408. https://doi.org/10.1016/j.bbamcr.2018.10.001.

33. Lambert H, Hitziger N, Dellacasa I, Svensson M, Barragan A. 2006. Induction of dendritic cell migration upon *Toxoplasma gondii* infection potentiates parasite dissemination. Cell Microbiol 8:1611–1623. https://doi.org/10.1111/j.1462-5822.2006.00735.x.

34. Kompalic-Cristo A, Frotta C, Suárez-Mutis M, Fernandes O, Britto C. 2007. Evaluation of a real-time PCR assay based on the repetitive B1 gene for the detection of *Toxoplasma gondii* in human peripheral blood. Parasitol Res 101:619–625. https://doi.org/10.1007/s00436-007-0524-9.